

Effect of pressure on the magnetostructural transition in SrFe₂As₂M. Kumar,^{1,*} M. Nicklas,^{1,†} A. Jesche,¹ N. Caroca-Canales,¹ M. Schmitt,¹ M. Hanfland,² D. Kasinathan,¹ U. Schwarz,¹ H. Rosner,¹ and C. Geibel¹¹Max Planck Institute for Chemical Physics of Solids, Nöthnitzer Strasse 40, 01187 Dresden, Germany²ESRF, BP 220, 38043 Grenoble Cedex 9, France

(Received 31 July 2008; revised manuscript received 17 September 2008; published 21 November 2008)

We present a systematic pressure study of poly- and single-crystalline SrFe₂As₂ by electrical-resistivity and x-ray-diffraction measurements. SrFe₂As₂ exhibits a structural phase transition from a tetragonal to an orthorhombic phase at $T_0=205$ K. The structural phase transition is intimately linked to a spin-density-wave transition taking place at the same temperature. Our pressure experiments show that T_0 shifts to lower temperatures with increasing pressure. We can estimate a critical pressure of 4–5 GPa for the suppression of T_0 to zero temperature. At pressures above 2.5 GPa the resistivity decreases significantly below $T_x \approx 40$ K, hinting at the emergence of superconductivity, but no zero-resistance state is observed up to 3 GPa.

DOI: [10.1103/PhysRevB.78.184516](https://doi.org/10.1103/PhysRevB.78.184516)

PACS number(s): 05.70.Ln, 71.20.Lp, 74.70.Dd, 75.30.Fv

I. INTRODUCTION

The recent discovery of superconductivity and the subsequent raising of the superconducting transition temperature T_c in iron arsenides has attracted tremendous interest in the scientific community. Superconductivity was first reported in RFeOAs compounds ($R=\text{La to Gd}$) (Refs. 1–5) and later on in the AFe₂As₂ series of compounds ($A=\text{Ca, Sr, Eu, Ba}$).^{6–9} The structures of both families of compounds present almost identical FeAs layers which are responsible for the peculiar behavior of these systems. The undoped compounds show a tetragonal-to-orthorhombic structural phase transition associated with magnetic ordering giving rise to a spin-density-wave instability between 150 and 200 K,^{6,7,10,11} which can be suppressed by chemical substitution or application of pressure.^{8,10,12} Doping-induced superconductivity was observed in fluorine-doped/O-depleted members of RFeOAs with T_c values approaching up to 50 K.^{1,2,5} The superconducting transition temperature reaches up to 38 K in AFe₂As₂ ($A=\text{Sr, Ba}$) on partial replacement of A with K or Cs.^{8,10,13} However, chemical substitution in contrast to the application of pressure changes not only the unit-cell volume but also the electronic structure considerably, for example, by adding or removing charge carriers from the conduction band.

In CaFe₂As₂ pressure studies reported a very fast suppression of the transition temperature T_0 related to the magnetic ordering and lattice distortion and its disappearance at around 0.4 GPa.^{12,14} Simultaneously, superconductivity appears with a maximum $T_c \approx 12$ K. Further on an anomaly appears above 0.5 GPa at around 100 K and shifts strongly to higher temperatures with increasing p . Neutron-scattering experiments evidenced this anomaly to correspond to a structural transition toward a collapsed tetragonal structure, with a reduced c/a ratio.¹⁵ In contrast measurements on BaFe₂As₂ revealed a much weaker pressure effect, with T_0 decreasing by only 15 K at 2 GPa, and no superconductivity until this pressure.¹⁶ A much weaker pressure effect for the larger alkaline-earth metals Sr and Ba was confirmed by Alireza *et al.*,¹⁷ who reported the onset of superconductivity at 2.8 and 2.5 GPa with maximum $T_c=27$ and 29 K for SrFe₂As₂ and BaFe₂As₂, respectively. However, one has to note that all

these results were obtained on single crystals grown from Sn flux. Especially in the case of BaFe₂As₂, this technique is known to lead to a significant incorporation of Sn into the single crystals, which strongly affects the physical properties, resulting, e.g., in a strong reduction in T_0 . On the other hand the huge difference between the pressure effect on CaFe₂As₂ and that on SrFe₂As₂ and BaFe₂As₂, as well as the absence of a collapsed phase in doped AFe₂As₂ (and doped RFeOAs), suggests that this collapsed phase might be unique to CaFe₂As₂, being related to the comparatively small size of Ca, and is not a general feature of the AFe₂As₂ materials. The absence of a collapsed phase in superconducting doped AFe₂As₂ already proves that this collapsed phase is neither a prerequisite for the disappearance of magnetic order nor that for the onset of superconductivity.

X-ray studies on SrFe₂As₂ at room temperature and down to 210 K evidenced an undistorted tetragonal ThCr₂Si₂-type structure, while at 205 K and below the diffraction diagrams can be well described by an orthorhombic unit cell in accordance with the proposed structure for BaFe₂As₂. Between 210 and 205 K, the high-temperature undistorted tetragonal phase disappears abruptly but a small amount of the orthorhombic phase coexists as expected for a first-order phase transition. Resistivity $\rho(T)$, susceptibility $\chi(T)$, and specific-heat $C(T)$ measurements show anomalies around 205 K.¹⁸ Our results on poly- and single-crystalline SrFe₂As₂ from high-pressure electrical-resistivity and x-ray-diffraction experiments reveal a suppression of T_0 with increasing pressure and hint at the possible existence of a magnetic instability in the pressure range from 4 to 5 GPa. Resistivity data suggest the emergence of a superconducting phase at $p > 2.5$ GPa.

II. METHODS

The polycrystalline SrFe₂As₂ samples were synthesized by heating a 1:2:2 mixture of Sr, Fe, and As in an Al₂O₃ crucible, sealing it under inert atmosphere inside an evacuated quartz tube and subsequent heating.⁷ Single crystals were obtained using the Bridgman method (cf. Ref. 9). Both types of samples crystallize in the undistorted tetragonal ThCr₂Si₂ structure. Measurements of the electrical resistance

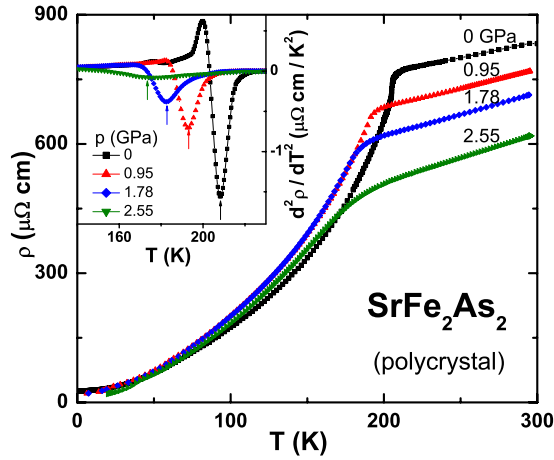


FIG. 1. (Color online) Electrical resistivity vs temperature for different pressures for polycrystalline SrFe_2As_2 . Inset: $d^2\rho(T)/dT^2$ for the same pressures; arrows indicate T_0 .

were carried out using a standard four-probe technique. A magnetic field was applied perpendicular to the current. The experiments on single crystals were made with current flowing in the (a, b) plane and magnetic field along the c direction. Temperatures down to 1.8 K and magnetic fields of up to 14 T were generated using a flow cryostat and a physical property measurement system (Quantum Design). Pressures of up to 3 GPa have been achieved in a double-layer piston-cylinder-type pressure cell with silicone oil as pressure-transmitting medium. The superconducting transition of Pb, which served as a pressure gauge, remained sharp at all pressures, indicating a pressure gradient less than 1–2 % of the applied pressure. The pressure change on cooling from room temperature to 1.8 K was less than 0.1 GPa. X-ray diffraction under pressure was conducted on ground crystalline powders of the compound. The samples were loaded into the gasket of a membrane-driven diamond anvil cell with a culet size of 0.6 mm. In order to realize hydrostatic conditions, helium was used as a pressure-transmitting medium. A helium gas-flow cryostat enabled thermostated low-temperature measurements. Sm-doped SrB_4O_7 was used as a temperature-insensitive pressure calibrant.^{19,20} Diffraction data were collected on ID9A at the ESRF, Grenoble, using a wavelength of 41.34 pm. During exposure, samples were oscillated by 6° in order to enhance powder statistics. Finally, the recorded two-dimensional (2D) diffraction patterns were integrated by means of the computer program FIT2D.²¹ To study the pressure dependence of the magnetic instability, band-structure calculations have been carried out within the local- (spin-) density approximation [L(S)DA], fixing the As z parameter to the experimental ambient-pressure values. We applied the full-potential local-orbital code FPLO (Ref. 22) (V 7.00-28) with the Perdew-Wang exchange-correlation potential²³ and a well-converged k mesh of 24^3 points for the Brillouin zone.

III. RESULTS AND DISCUSSION

Figure 1 shows the electrical resistivity of polycrystalline

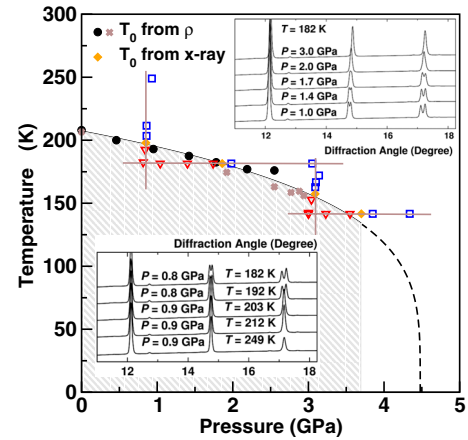


FIG. 2. (Color online) Temperature-pressure phase diagram of SrFe_2As_2 with T_0 values from the evaluation of resistivity data (polycrystal—filled circles; single crystal—stars) and x-ray measurements (filled diamonds). The data points for the x-ray measurements are shown as open squares and triangles for the tetragonal and the orthorhombic phases, respectively. The approximately isobaric and isothermic runs are guided by horizontal and vertical lines. Exemplary x-ray patterns are presented in the upper and lower insets. The splitting of the reflections at about 15° and 17° indicates the structural transition. The measured region for the orthorhombic (magnetic) phase is shaded in gray. The dashed line is an extrapolation of the phase boundary down to zero temperature.

SrFe_2As_2 as a function of temperature for selected pressures. At ambient pressure $\rho(T)$ is weakly decreasing between 300 and 205 K. At around 205 K $\rho(T)$ shows a sharp drop at T_0 followed by a further strong decrease to low temperatures, in quite good agreement with the previously reported $T_0 = 198$ K.²⁴ On increasing pressure the feature at T_0 becomes broader but is still well defined up to the highest pressure of our electrical-resistivity experiment. There is no qualitatively different behavior between the polycrystalline and the single-crystalline materials. At ambient pressure the polycrystals have a residual resistivity ratio of $RR_{1.8\text{ K}} = \rho_{300\text{ K}}/\rho_{1.8\text{ K}} = 32$ and a room-temperature resistivity $\rho_{300\text{ K}} = 0.83$ m Ω cm compared with $RR_{1.8\text{ K}} = 25$ and $\rho_{300\text{ K}} = 1.09$ m Ω cm for the single crystals. However, the kink at T_0 remains sharper for the single crystal at high pressure. It is also worth mentioning that magnetic field of $B = 9$ T has no effect on T_0 in the single-crystalline sample at our highest pressure of 2.94 GPa for $B \parallel c$, similar to the behavior reported at ambient pressure.²⁴ T_0 as defined by the minimum in the second derivative $d^2\rho(T)/dT^2$ (cf. inset of Fig. 1) shifts toward lower temperatures on application of pressure. The phase diagram in Fig. 2 summarizes the results. Within the error bars there is no difference between the poly- and single-crystalline samples. Initially $T_0(p)$ decreases with a slope of $dT_0/dp|_{p=0} \approx -13$ K/GPa with increasing pressure. $dT_0/dp|_{p=0}$ of SrFe_2As_2 is in fairly good agreement with $dT_0/dp|_{p=0} \approx -10.4$ K/GPa reported for BaFe_2As_2 (Ref. 16) but almost one order of magnitude smaller than for CaFe_2As_2 .¹²

In the AFe_2As_2 compounds, T_0 at ambient pressure corresponds to both the structural transition and the onset of antiferromagnetic ordering, which are intimately linked

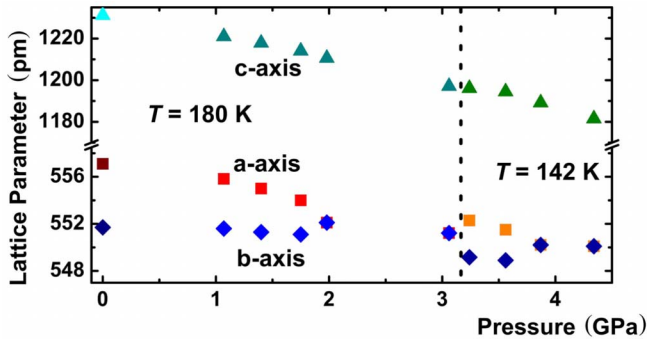


FIG. 3. (Color online) Lattice parameters as refined from x-ray-diffraction data collected at different temperatures and pressures. Coincidence of the parameters a and b indicates the tetragonal phase.

together.^{7,18} In contrast, it is presently suggested that in the $R\text{FeOAs}$ compounds,⁴ the antiferromagnetic ordering occurs at approximately 10–20 K below the structural ordering. There both transitions are marked by an anomaly in the resistivity.⁴ A careful analysis of our resistivity data do not reveal any evidence for a splitting of the anomaly at T_0 under pressure, neither in $\rho(T)$ nor in its first or second derivative. Thus our resistivity data evidence that both transitions remain linked together under pressure. In order to get additional information on the effect of pressure on this transition, we carried out temperature-dependent high-pressure x-ray-diffraction studies for pressures of up to 4.4 GPa and temperatures down to 140 K. We performed two approximately isothermal and isobaric runs, respectively. Exemplary x-ray patterns are presented in the insets of Fig. 2, and the lattice parameters of the isothermal measurements are presented in Fig. 3. For each run, we could observe a clear phase transition from the tetragonal to the orthorhombic phase with decreasing temperature or a suppression of the distortion with increasing pressure. The phase boundary has been determined as the midpoint (filled diamonds in Fig. 2) between the boundary points of the two phases.

At 2.55 GPa a sharp decrease in resistivity shows up below 40 K in the data of the polycrystalline sample. In the single crystal a similar reduction is observed at a slightly higher pressure ($p=2.88$ GPa) and at somewhat lower temperature. However, we do not observe zero resistance at any pressure investigated in this study. The transition temperature T_x is in the same range where electron-doped SrFe_2As_2 becomes superconducting, giving a hint of a superconducting origin of the reduced resistance below T_x .²⁵ To further elucidate the nature of the transition observed in the electrical resistivity, we applied a magnetic field. The results at $p=2.55$ GPa for the polycrystalline sample and at $p=2.94$ GPa for the single-crystalline sample are presented in Fig. 4. With increasing magnetic field the reduction in the resistivity becomes smaller and the T_x shifts in the whole accessible magnetic-field range toward lower temperatures. Up to 14 T $B_x(T)=B(T=T_x)$ depends linearly on the temperature and the initial slope $dB_x(T)/dT|_{T=T_x}=-2.05$ T/K, the same for both samples and pressures, is typical of the superconducting upper critical field $B_{c2}(T)$ in the iron arsenide

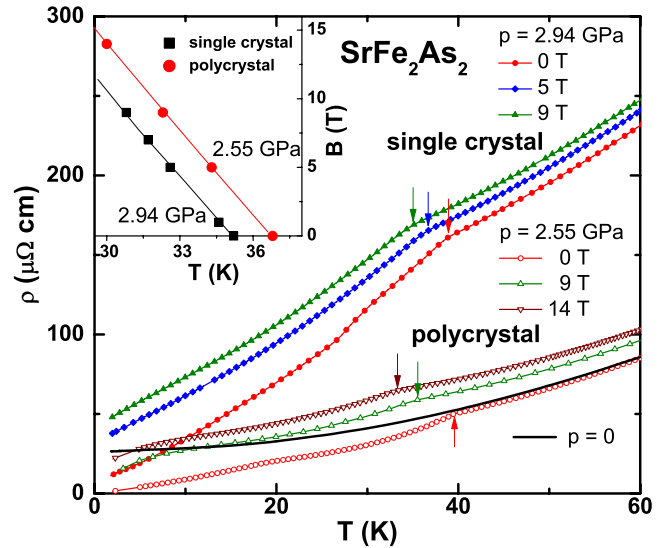


FIG. 4. (Color online) Electrical resistivities of SrFe_2As_2 at $p=2.55$ GPa (polycrystal, open symbols) and at $p=2.94$ GPa (single crystal, solid symbols) in different applied magnetic fields. The solid line represents the ambient-pressure data for the polycrystalline sample as a reference. The arrows indicate T_x . Inset: B - T diagram compiled from the resistivity data.

compounds.¹² From these indications we speculate that the observed drop in the electrical resistivity indicates the emergence of a superconducting phase in SrFe_2As_2 .

Comparing the phase boundary constructed from the x-ray-diffraction and the electrical-resistivity data for both poly- and single-crystalline samples, we find excellent agreement between all measurements. Thus, we clearly observe an orthorhombic phase for pressures below 3.8 GPa and $T < 140$ K. At ambient pressure, the occurrence of the orthorhombic phase is intimately linked to antiferromagnetism. According to our electronic structure calculations, this intimate connection between the antiferromagnetic order and the orthorhombic distortion is preserved under pressure. Simulating hydrostatic pressure in our calculations, we find that the magnetic instability disappears at about 10% volume reduction, corresponding to a critical pressure of slightly more than 10 GPa. This value should be considered as a rough upper estimate since it suffers from the known LDA overestimate of magnetism in this class of compounds. In contrast to CaFe_2As_2 , where our calculations indicate the tetragonal collapsed phase similar to that in Ref. 15, we find no such transition for AFe_2As_2 ($A=\text{Sr}, \text{Ba}, \text{Eu}$). This suggests that the c/a collapse of the tetragonal phase is a rather special feature of the CaFe_2As_2 system without general relevance for the phase diagram of the AFe_2As_2 compound family. A more precise study, including the pressure dependence of the magnetic transition upon doping, will be the subject of future investigation.²⁶ Our preliminary results indicate a considerable influence of doping and impurities on the critical pressure. This result, although preliminary, may offer an explanation for the observed differences in transition pressures in different samples.^{12,14,17}

Results from specific-heat, magnetic-susceptibility, and resistivity experiments,⁷ as well as x-ray, neutron-diffraction,

muon-spin-relaxation, and Mössbauer experiments, indicate a first-order nature of the transition at T_0 .¹⁸ However, Tegel *et al.*²⁷ concluded a second-order type of the transition from their temperature-dependent x-ray powder diffraction and Mössbauer spectroscopy. To get a further insight into the nature of the phase transition, we analyzed the slope of our $T_0(p)$ data at $p=0$ utilizing the Clausius-Clapeyron equation $dT/dp=T\Delta V/\Delta H$ applicable for a first-order phase transition. With the initial slope $dT/dp=-13$ K/GPa and the latent heat at the transition, $\Delta H\approx 200$ J/mol,¹⁸ we obtain a volume change for the orthorhombic unit cell, $\Delta V=-0.8\times 10^{-4}$ nm³, which has the same sign and the same order of magnitude as the experimental result of $\Delta V=-0.3\times 10^{-4}$ nm³.²⁷ An analysis for a second-order transition leads to a discrepancy of at least 1 order of magnitude between calculated and observed specific-heat anomalies. Therefore this comparison supports the first-order nature of the transition.

IV. SUMMARY AND CONCLUSION

In summary, we have determined the effect of pressure on the structural and magnetic transition in SrFe₂As₂ using electrical-resistivity and x-ray-diffraction measurements. We observe a weak decrease in T_0 with increasing pressure with an initial slope of -13 K/GPa and a bending toward lower temperatures at higher pressures. Extrapolating these data and assuming a continuous suppression of T_0 down to $T=0$ would lead to a critical pressure on the order of 4.5 GPa. However, the suspected first-order nature of the phase transition at T_0 makes a classical critical end point at a finite

temperature more likely. We still observe a transition to the orthorhombic phase at 3.8 GPa below 140 K. Nevertheless already at around 2.5 GPa we observed in $\rho(T)$ a kink at 40 K leading to a stronger slope $d\rho(T)/dT$ at lower temperatures. This is suggestive of superconductivity emerging at the disappearance of the structural and magnetic transition. This interpretation is supported by the linear shift of this anomaly to lower temperatures with applied magnetic field. These experimental observations are supported by results of band-structure calculations, which also indicate that the antiferromagnetic order becomes unstable upon volume reduction. Thus, in contrast to the observation in the high-temperature superconductors based on cuprates, in the layered FeAs systems the suppression of magnetism and the onset of superconductivity do not need electron or hole doping but can be achieved without doping by tuning the electronic states with pressure. The suppression of magnetism upon applying pressure is in accordance with and a further hint of an itinerant character of the magnetism since for localized magnetism one usually expects an enhancement of the ordering temperature with pressure.

Note added. Recently we learned of a paper presenting a resistivity study of SrFe₂As₂ in the pressure range of up to 2 GPa.²⁸ In this work a similar decrease in $\rho(T)$ below T_x , which we observe only above 2.5 GPa, is reported at smaller pressure.

ACKNOWLEDGMENT

It is a pleasure to thank K. Meier for the support of the x-ray-diffraction measurements.

*manoj.kumar@cpfs.mpg.de

†nicklas@cpfs.mpg.de

¹Y. Kamihara, T. Watanabe, M. Hirano, and H. Hosono, *J. Am. Chem. Soc.* **130**, 3296 (2008).

²X. F. Chen, T. Wu, G. Wu, R. H. Liu, H. Chen, and D. F. Fang, *Nature (London)* **453**, 761 (2008).

³C. de La Cruz, Q. Huang, J. W. Lynn, Jiying Li, W. Ratcliff II, J. L. Zarestky, H. A. Mook, G. F. Chen, J. L. Luo, N. L. Wang, and P. Dai, *Nature (London)* **453**, 899 (2008).

⁴H. H. Klauss, H. Luetkens, R. Klingeler, C. Hess, F. J. Litterst, M. Kraken, M. M. Korshunov, I. Eremin, S. L. Drechsler, R. Khasanov, A. Amato, J. Hamann-Borrero, N. Leps, A. Kondrat, G. Behr, J. Werner, and B. Büchner, *Phys. Rev. Lett.* **101**, 077005 (2008).

⁵M. Fratini, R. Caivano, A. Puri, A. Ricci, Z. A. Ren, X. L. Dong, J. Yang, W. Lu, Z. X. Zhao, L. Barba, G. Arrighetti, M. Polentarutti, and A. Bianconi, *Supercond. Sci. Technol.* **21**, 092002 (2008).

⁶N. Ni, S. Nandi, A. Kreyssig, A. I. Goldman, E. D. Mun, S. L. Bud'ko, and P. C. Canfield, *Phys. Rev. B* **78**, 014523 (2008).

⁷C. Krellner, N. Caroca-Canales, A. Jesche, H. Rosner, A. Ormeci, and C. Geibel, *Phys. Rev. B* **78**, 100504(R) (2008).

⁸M. Rotter, M. Tegel, D. Johrendt, I. Schellenberg, W. Hermes, and R. Pöttgen, *Phys. Rev. B* **78**, 020503(R) (2008).

⁹H. S. Jeevan, Z. Hossain, D. Kasinathan, H. Rosner, C. Geibel,

and P. Gegenwart, *Phys. Rev. B* **78**, 052502 (2008).

¹⁰K. Sasmal, B. Lv, B. Lorenz, A. M. Guloy, F. Chen, Y. Y. Xue, and C. W. Chu, *Phys. Rev. Lett.* **101**, 107007 (2008).

¹¹G. F. Chen, Z. Li, J. Dong, G. Li, W. Z. Hu, X. D. Zhang, X. H. Song, P. Zheng, N. L. Wang, and J. L. Luo, arXiv:0806.2648 (unpublished).

¹²M. S. Torikachvili, S. L. Bud'ko, N. Ni, and P. C. Canfield, *Phys. Rev. Lett.* **101**, 057006 (2008).

¹³G. F. Chen, Z. Li, G. Li, W. Z. Hu, J. Dong, X. D. Zhang, P. Zheng, N. L. Wang, and J. L. Luo, *Chin. Phys. Lett.* **25**, 3403 (2008).

¹⁴T. Park, E. Park, H. Lee, T. Klimczuk, E. D. Bauer, F. Ronning, and J. D. Thompson, *J. Phys.: Condens. Matter* **20**, 322204 (2008).

¹⁵A. Kreyssig, M. A. Green, Y. Lee, G. D. Samolyuk, P. Zajdel, J. W. Lynn, S. L. Bud'ko, M. S. Torikachvili, N. Ni, S. Nandi, J. Leão, S. J. Poulton, D. N. Argyriou, B. N. Harmon, P. C. Canfield, R. J. McQueeney, and A. I. Goldman, arXiv:0807.3032 (unpublished).

¹⁶M. S. Torikachvili, N. Ni, S. L. Bud'ko, and P. C. Canfield, arXiv:0807.1089 (unpublished).

¹⁷P. L. Alireza, J. Gillett, Y. T. C. Ko, S. E. Sebastian, and G. G. Lonzarich, arXiv:0807.1896, *J. Phys.: Condens. Matter* (to be published).

¹⁸A. Jesche, N. Caroca-Canales, H. Rosner, H. Borrmann, A. Or-

- meci, D. Kasinathan, K. Kaneko, H. H. Klauss, H. Luetkens, R. Khasanov, A. Amato, A. Hoser, C. Krellner, and C. Geibel, *Phys. Rev. B* **78**, 180504 (2008).
- ¹⁹A. Lacam and C. Chateau, *J. Appl. Phys.* **66**, 366 (1989).
- ²⁰F. Datchi, R. LeToullec, and P. Loubeyre, *J. Appl. Phys.* **81**, 3333 (1997).
- ²¹A. P. Hammersley, S. O. Svensson, M. Hanfland, A. Fitch, and D. Häusermann, *High Press. Res.* **14**, 235 (1996).
- ²²K. Koepnik and H. Eschrig, *Phys. Rev. B* **59**, 1743 (1999).
- ²³J. P. Perdew and Y. Wang, *Phys. Rev. B* **45**, 13244 (1992).
- ²⁴J. Q. Yan, A. Kreyssig, S. Nandi, N. Ni, S. L. Bud'ko, A. Kracher, R. J. McQueeney, R. W. McCallum, T. A. Lograsso, A. I. Goldman, and P. C. Canfield, *Phys. Rev. B* **78**, 024516 (2008).
- ²⁵A. Leithe-Jasper, W. Schnelle, C. Geibel, and H. Rosner, *Phys. Rev. Lett.* **101**, 207004 (2008).
- ²⁶D. Kasinathan, A. Ormeci, M. Schmitt, M. Kumar, C. F. Miclea, M. Nicklas, M. Hanfland, K. Koch, U. Schwarz, H. S. Jeevan, P. Gegenwart, A. Jesche, C. Krellner, N. Caroca-Canales, Z. Hos-sain, C. Geibel, W. Schnelle, A. Leithe-Jasper, and H. Rosner (unpublished).
- ²⁷M. Tegel, M. Rotter, V. Weiss, F. M. Schappacher, R. Pöttgen, and D. Johrendt, arXiv:0806.4782 (unpublished).
- ²⁸M. S. Torikachvili, S. L. Bud'ko, N. Ni, and P. C. Canfield, *Phys. Rev. B* **78**, 104527 (2008).